Structure and Optical Properties of Several Organic−Inorganic Hybrids Containing Corner-Sharing Chains of Bismuth Iodide Octahedra

David B. Mitzi*,† and Phillip Brock‡

IBM T. J. Watson Research Center, P.O. Box 218, Yorktown Heights, New York 10598, and IBM Almaden Research Center, 650 Harry Road, San Jose, California 95120

Two organic−inorganic bismuth iodides of the form $(H_3N-R-NH_3)BiI_5$ are reported, each containing long and relatively flexible organic groups, R. The inorganic framework in each case consists of distorted BiI_6 octahedra sharing cis vertexes to form zigzag chains. Crystals of $(H_3NC_{18}H_{24}S_2NH_3)BiI_5$ were grown from a slowly cooled ethylene glycol/2-butanol solution containing bismuth(III) iodide and AETH·2HI, where AETH = 1,6-bis[5′-(2″-aminoethyl)-2′-thienyl]hexane. The new compound, $(H_2AETH)BiI_5$, adopts an orthorhombic (*Aba*2) cell with the lattice parameters $a = 20.427(3)$ Å, $b = 35.078(5)$ Å, $c = 8.559(1)$ Å, and $Z = 8$. The structure consists of corrugated layers of BiI_5^{2-} chains, with Bi−I bond lengths ranging from 2.942(3) to 3.233(3) Å, separated by layers of the organic $(H_2AETH)^{2+}$ cations. Crystals of the analogous $(H_3NC_{12}H_{24}NH_3)BiI_5$ compound were also prepared from a concentrated aqueous hydriodic acid solution containing bismuth(III) iodide and the 1,12-dodecanediamine (DDDA) salt, DDDA·2HI. $(H_2DDDA)BiI_5$ crystallizes in an orthorhombic (*Ibam*) cell with $a = 17.226(2)$ Å, $b = 34.277(4)$ Å, $c = 8.654(1)$ Å, and $Z = 8$. The Bi−I bonds range in length from 2.929(1) to 3.271(1) Å. While the inorganic chain structure is nearly identical for the two title compounds, as well as for the previously reported $(H_3NC_6H_{12}NH_3)BiI_5$ [i.e., $(H_2DAH)BiI_5$] structure, the packing of the chains is strongly influenced by the choice of organic cation. Optical absorption spectra for thermally ablated thin films of the three organic−inorganic hybrids containing BiI_5^{2-} chains are reported as a function of temperature (25−290 K). The dominant long-wavelength feature in each case is attributed to an exciton band, which is apparent at room temperature and, despite the similar inorganic chain structure, varies in position from 491 to 541 nm (at 25 K).

Introduction

Organic−inorganic hybrids provide an exciting opportunity to combine useful attributes of organic and inorganic materials within a single molecular scale composite. The hybrid perovskites, for example, are a relatively large structural family in which a number of interesting magnetic, optical, and electrical phenomena have recently been observed as a result of the integration of organic and inorganic components.[1] These and other related systems generally consist of one-, two-, or three-dimensional networks of corner-sharing divalent metal halide octahedra, separated by organic cations. For relatively simple, unconjugated, organic molecules, the organic component can be used as a physical and electronic barrier, which insulates or sheathes the lower dimensional inorganic framework. For more complex conjugated molecules, the organic component contributes more actively to the electrical and optical properties.[2] Because of the interesting characteristics that arise in these lower dimensional systems,[1,3] as well as the relative ease with which the metal halide based hybrids can be processed at near-ambient temperatures, organic−inorganic perovskites are candidates for electronic and optoelectronic devices.[4−7]

While the perovskites are one of the most extensive families of organic−inorganic hybrids, a variety of other metal halide based systems exhibit a similar range of potentially interesting properties. Of these, bismuth iodide based hybrids are interesting because of the potentially semiconducting character of the inorganic framework,[8,9] as well as the rich structural diversity displayed by these systems. Bismuth halide lattices generally consist of octahedrally coordinated bismuth, with the octahedra exhibiting a varying degree of distortion. The BiI_6 octahedra may join to form discrete (i.e., mononuclear) or extended (i.e., polynuclear) inorganic networks of corner-, edge-, or face-sharing octahedra, leading to an extensive family of bismuth halogenoanions (e.g., BiX_4^-, BiX_5^{2-}, BiX_6^{3-}, $Bi_2X_9^{3-}$, $Bi_2X_{11}^{5-}$, $Bi_3X_{12}^{3-}$, $Bi_4X_{18}^{6-}$, $Bi_5X_{18}^{3-}$, $Bi_6X_{22}^{4-}$, and $Bi_8X_{30}^{6-}$).[10] Among the bismuth iodides, isolated BiI_6 octahedra are found in $(C_6H_5-CH_2CH_2NH_3)_4BiI_7 \cdot H_2O$,[11] with iodide anions and water molecules interposed between the octahedra in the inorganic layers of the structure. Chains of corner-sharing octahedra are found in $(H_3NC_6H_{12}NH_3)BiI_5$.[12] In (2-picolinium)BiI_4 and (quinolinium)BiI_4, the polymeric inorganic anion is built up from edge-

---

   * To whom correspondence should be addressed.
   † IBM T. J. Watson Research Center.
   ‡ IBM Almaden Research Center.
(1) For a recent review, see: Mitzi, D. B. *Prog. Inorg. Chem.* **1999**, *48*, 1.
(2) Mitzi, D. B.; Chondroudis, K.; Kagan, C. R. *Inorg. Chem.* **1999**, *38*, 6246.
(3) For a recent review, see: Papavassiliou, G. C. *Prog. Solid State Chem.* **1997**, *25*, 125.
(4) Chondroudis, K.; Mitzi, D. B. *Chem. Mater.* **1999**, *11*, 3028.
(5) Kagan, C. R.; Mitzi, D. B.; Dimitrakopoulos, C. D. *Science* **1999**, *286*, 945.
(6) Era, M.; Morimoto, S.; Tsutsui, T.; Saito, S. *Appl. Phys. Lett.* **1994**, *65*, 676.
(7) Mitzi. D. B.; Chondroudis, K.; Kagan, C. R. *IBM J. Res. Dev.* **2001**, *45*, 29.
(8) Belotskii, D. P.; Timofeev, V. B.; Antipov, I. N.; Vashchenko, V. I.; Bespal'chenko V. A. *Russ. J. Phys. Chem.* **1968**, *42*, 740.
(9) Fischer, G. *Helv. Phys. Acta* **1961**, *34*, 827.
(10) Fisher, G. A.; Norman, N. C. *Adv. Inorg. Chem.* **1994**, *41*, 233.
(11) Papavassiliou, G. C.; Koutselas, I. B.; Terzis, A.; Raptopoulou, C. P. *Z. Naturforsch.* **1995**, *50b*, 1566.

sharing BiI$_6$ octahedra,[13,14] while in (Ph$_4$P)$_3$Bi$_5$I$_{18}$, the anion consists of a linear chain of five face-sharing octahedra.[15] Extensive work has also been done on the Bi$_2$I$_9^{3-}$ family of compounds, which generally consist of isolated pairs of face-sharing BiI$_6$ octahedra.[16,17] Recently, a layered perovskite of the form [H$_2$AEQT]Bi$_{2/3}$I$_4$ [AEQT = 5,5‴-bis(aminoethyl)-2,2′: 5′,2″:5″,2‴-quaterthiophene] has been reported,[18] with layers of rigid, rodlike AEQT cations templating the unusual metal-deficient inorganic sheets.

Members of the organic−inorganic bismuth iodide family with extended or polymeric inorganic frameworks are of particular interest because of the possibility of semiconducting electronic character. In this respect, the (H$_3$NC$_6$H$_{12}$NH$_3$)BiI$_5$ compound [i.e., (H$_2$DAH)BiI$_5$, where DAH = diaminohexane] reported recently by Mousdis et al.[12] is an important model compound. The structure consists of one-dimensional zigzag chains of corner-sharing BiI$_6$ octahedra, similar to those found in (piperidinium)$_2$BiBr$_5$[19] and (4,4′-bipyridinium)SbCl$_5$.[20] The optical features (e.g., band edge and exciton peak position) of the one-dimensional (H$_2$DAH)BiI$_5$ compound are intermediate in position relative to the zero-dimensional A$_3$BiI$_6$ (A = organic cation) and two-dimensional BiI$_3$ compounds, suggesting that the structural distinction between extended 0D, 1D, and 2D systems carries over to the electronic properties of the material as well.[12]

In an effort to probe the structural flexibility of these chain-based bismuth(III) iodide systems and the effect of new organic cations on the structure and properties of the inorganic framework, we examine two new compounds of the form (H$_3$N−R−NH$_3$)BiI$_5$, with longer and more complex organic groups, R.

Experimental Section

Synthesis. (H$_2$AETH)BiI$_5$ Crystals. (H$_2$AETH)BiI$_5$ crystals were grown from a slowly cooled, slightly acidified, 2-butanol/ethylene glycol solution containing the organic and inorganic salts. First, 59.2 mg (0.10 mmol) of AETH·2HI and 59.0 mg (0.10 mmol) of freshly sublimed BiI$_3$ were weighed and added to a test tube under an inert atmosphere. The contents were dissolved in the sealed tube at 120 °C in a solvent mixture of 3 mL of 2-butanol, 0.3 mL of ethylene glycol, and 2 drops of 57% aqueous HI, forming a nominally saturated solution. Upon slow cooling at 4 °C/h to −20 °C, thin, red, platelike crystals of the title (H$_2$AETH)BiI$_5$ compound formed (108 mg; 0.09 mmol). The crystals were rinsed with 2-propanol, filtered and dried under vacuum, and stored in an argon-filled glovebox with oxygen and water levels maintained below 1 ppm. Chemical analysis of the (C$_{18}$H$_{30}$S$_2$N$_2$)BiI$_5$ crystals: theory [C (18.29%), H (2.56%), N (2.37%)]; found [C (18.5%), H (2.7%), N (2.2%)].

(H$_2$DDDA)BiI$_5$ Crystals. (H$_2$DDDA)BiI$_5$ crystals were grown from a slowly cooled, saturated, aqueous hydriodic acid solution containing the organic and inorganic salts. First, 36.5 mg (0.08 mmol) of DDDA· 2HI and 47.2 mg (0.08 mmol) of freshly sublimed BiI$_3$ were weighed and added to a test tube under an inert atmosphere. The contents were dissolved in the sealed tube at 125 °C in 2 mL of concentrated (57 wt %) aqueous hydriodic acid. Upon cooling at 3 °C/h to −10 °C, thin, red, elongated plates of the desired (H$_2$DDDA)BiI$_5$ compound formed (61 mg; 0.06 mmol), along with a small amount of an unidentified white powdery material (possibly DDDA·2HI). The white material was washed from the red crystals using 2-propanol. The (H$_2$DDDA)BiI$_5$ crystals were subsequently stored in an argon-filled glovebox. Chemical analysis of the (C$_{12}$H$_{30}$N$_2$)BiI$_5$ crystals: theory [C (13.78%), H (2.89%), N (2.68%)]; found [C (13.8%), H (2.7%), N (2.7%)].

Attempts to grow crystals of (H$_2$DDDA)BiI$_5$ using an ethylene glycol/2-butanol mixture, as described above for (H$_2$AETH)BiI$_5$, led to long red needlelike crystals, which preliminary analysis revealed to be a distinct compound based on isolated Bi$_2$I$_9^{3-}$ anions. This phase appears to be quite stable in the ethylene glycol/2-butanol solution since, even when the ratio of DDDA·2HI to BiI$_3$ was varied, the same compound formed. This phase was not, however, identified in reactions carried out in concentrated hydriodic acid.

Thin Film Deposition. Films of (H$_2$AETH)BiI$_5$ and (H$_2$DDDA)-BiI$_5$ were prepared for optical measurement using the single source thermal ablation (SSTA) technique.[21,22] The substrates (quartz/sapphire) were cleaned by sonication in toluene (20 min), followed by sonication in acetone (20 min), and methanol (20 min). They were subsequently placed in a 110 °C oven to dry. A suspension [for (H$_2$AETH)BiI$_5$] or solution [for (H$_2$DDDA)BiI$_5$] of the bismuth iodide salt was made by adding 10 mg of the salt to 0.1 mL of methanol, followed by sonication for 15 min. For (H$_2$AETH)BiI$_5$, a stoichiometric charge was used, while for (H$_2$DDDA)BiI$_5$, the addition of an 8 mg excess DDDA·2HI was found to improve the phase purity of the desired final film. Note that the suspension can consist of either the single hybrid compound or a stoichiometric mixture of the two component salts. Since the ablation process is essentially instantaneous, only the overall stoichiometry on the heater sheet is important.

The suspension (or solution) was placed dropwise via a syringe on the tantalum heater of the SSTA chamber. The chamber was then closed and evacuated with a rotary mechanical pump until all the solvent evaporated (typically about 2 min). A turbomolecular pump was then switched on and the system was pumped to approximately 10^{-7} Torr. After closing the gate valve to the pumping system (i.e., creating a static vacuum), a large current of approximately 90 A was passed through the heater for about 5 s, leading to an essentially instantaneous ablation of the organic−inorganic hybrid. The deposited (H$_2$AETH)-BiI$_5$ [(H$_2$DDDA)BiI$_5$] films were thermally annealed at 115 °C [80 °C] for 20 min on a digitally controlled hot plate within a nitrogen-filled glovebox. These annealing temperatures yielded films with reasonably strong X-ray diffraction patterns (Figure 1). For comparison, films of (H$_2$DAH)BiI$_5$ were also deposited using similar parameters.[21] In contrast to the two new compounds, which form highly oriented films, the deposited (H$_2$DAH)BiI$_5$ films do not have a substantially preferred orientation. This difference in film formation suggests that the (H$_2$-AETH)BiI$_5$ and (H$_2$DDDA)BiI$_5$ structures are more layerlike in character, compared to the (H$_2$DAH)BiI$_5$ structure (as confirmed by the structural analysis described below). Furthermore, the full range of indexed (*hkl*) reflections for the (H$_2$DAH)BiI$_5$ system enables a rigorous confirmation that the thin film crystal structure is the same as that for the bulk. Film thicknesses for each of the compounds, measured with a Tencor Instruments Alpha-Step 200, varied between approximately 400 and 700 Å.

X-ray Crystallography. A red (H$_2$AETH)BiI$_5$ [(H$_2$DDDA)BiI$_5$] crystal, with the approximate dimensions 0.01 mm × 0.10 mm × 0.23 mm [0.01 mm × 0.04 mm × 0.34 mm], was selected under a microscope and attached to the end of a quartz fiber with 5 min epoxy. A full sphere of data was collected at room temperature on a Bruker SMART CCD diffractometer, equipped with a normal focus 2.4 kW sealed tube X-ray source (Mo Kα radiation). Intensity data were collected with a detector distance of approximately 5.0 cm, in 2272 frames with increasing ω, and an exposure time of 240 s [200 s] per frame. The increment in ω between each frame was 0.3°. The initial

(12) Mousdis G. A.; Papavassiliou, G. C.; Terzis, A.; Raptopoulou, C. P. *Z. Naturforsch.* **1998**, *53b*, 927.

(13) Robertson, B. K.; McPherson, W. G.; Meyers, E. A. *J. Phys. Chem.* **1967**, *71*, 3531.

(14) Nagapetyan, S. S.; Arakelova, A. R.; Ziger, E. A.; Koshkin, V. M.; Struchkov, Y. T.; Shklover, V. E. *Russ. J. Inorg. Chem.* **1989**, *34*, 1276.

(15) Pohl, S.; Peters, M.; Haase, D.; Saak, W. *Z. Naturforsch.* **1994**, *49b*, 741.

(16) Lazarini, F. *Acta Crystallogr., Sect. C* **1987**, *C43*, 875.

(17) Gridunova, G. V.; Ziger, E. A.; Koshkin, V. M.; Struchkov, Y. T.; Shklover, V. E. *Russ. J. Inorg. Chem.* **1988**, *33*, 977.
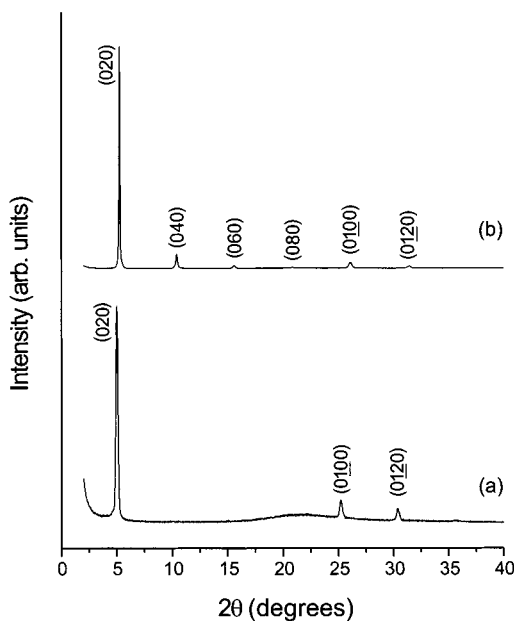
(18) Mitzi, D. B. *Inorg. Chem.* **2000**, *39*, 6107.

(19) McPherson, W. G.; Meyers, E. A. *J. Phys. Chem.* **1968**, *72*, 532.

(20) Lipka, A. *Z. Naturforsch.* **1983**, *38b*, 1615.

(21) Mitzi, D. B.; Prikas, M. T.; Chondroudis, K. *Chem. Mater.* **1999**, *11*, 542.

(22) Chondroudis, K.; Mitzi, D. B.; Brock, P. *Chem. Mater.* **2000**, *12*, 169.

Figure 1. Room temperature X-ray diffraction patterns for thin films of (a) $(H_2AETH)BiI_5$ and (b) $(H_2DDDA)BiI_5$, deposited using the SSTA technique and annealed for 20 min at 115 and 80 °C, respectively. The reflection indices are shown for each pattern. For the $(H_2AETH)BiI_5$ film, the derived *b*-axis lattice parameter from the observed reflections is $b = 35.2(1)$ Å, while for $(H_2DDDA)BiI_5$, the value is $b = 34.1(1)$ Å.

orthorhombic unit cell was selected for each compound based on an indexing of 522 [974] reflections. The final unit cell parameters and crystal orientation matrix were obtained by a least-squares fit of 8192 reflections. An empirical absorption correction, based on equivalent reflections, was applied to the intensity data.[23]

The structure was solved and refined using the NRCVAX 386 PC version program.[24] First, the Bi and I atoms were located using direct methods. The S, N, and C atoms were then located using successive Fourier difference maps. All heavy atoms (Bi, I, and S) were refined anisotropically. The thermal ellipsoids of the carbon atoms were, in general, quite large, and therefore the organic components were refined isotropically. No attempts were made to locate the hydrogen atoms. The minimum and maximum peaks in the final difference Fourier maps corresponded to -1.33 and 1.67 e/Å^3 [-0.73 and 1.06 e/Å^3]. For $(H_2$-AETH$)BiI_5$, the first five residual peaks all appeared within approximately 1 Å of a heavy atom (Bi or I). For $(H_2DDDA)BiI_5$, the first residual peak was approximately 0.6 Å from I(3). Two peaks from the first five residual peaks were close to carbon atoms from the dodecane chain. No additional symmetry was detected for either compound using the MISSYM program.[25] Selected crystallographic results for both compounds are summarized in Table 1. The atomic coordinates for $(H_2AETH)BiI_5$ and $(H_2DDDA)BiI_5$ are listed in Tables 2 and 3, respectively. Selected bond distances and angles are provided for each compound in Tables 4 and 5. A complete listing of crystallographic data, along with anisotropic displacement parameters for each compound, is given as Supporting Information.

Optical Properties. Absorption spectra were obtained on thermally ablated films (deposited on sapphire disks) of $(H_2AETH)BiI_5$, $(H_2$-DDDA$)BiI_5$, and $(H_2DAH)BiI_5$, using a Hewlett-Packard UV–vis 8543 spectrophotometer. The sapphire disks were mounted on a coldfinger and cooled with an APD Cryogenics displex system. A pressed indium O-ring contact was used between the sapphire and copper coldfinger to improve thermal contact. Measurements were made over the temperature range 25–290 K.

(23) Sheldrick, G. M. *SADABS*; Institut für Anorganische Chemie der Universität Göttingen: Göttingen, 1997.

(24) Gabe, E. J.; Le Page, Y.; Charland, J.-P.; Lee, F. L.; White, P. S. *J. Appl. Crystallogr.* **1989**, *22*, 384.

(25) Le Page, Y. *J. Appl. Crystallogr.* **1988**, *21*, 983.

Table 1. Room Temperature Crystallographic Data for $(H_2AETH)BiI_5$ and $(H_2DDDA)BiI_5$

chemical formula	$C_{18}H_{30}S_2N_2BiI_5$	$C_{12}H_{30}N_2BiI_5$
fw	1182.08	1045.89
space group	*Aba2* (No. 41)	*Ibam* (No. 72)
a, Å	20.427(3)	17.226(2)
b, Å	35.078(5)	34.277(4)
c, Å	8.559(1)	8.654(1)
V, Å^3	6133(1)	5110(1)
Z	8	8
ρ_{calcd}, g/cm^3	2.561	2.719
wavelength (Å)	0.71073 (Mo Kα)	0.71073 (Mo Kα)
abs coeff (μ), cm^{-1}	109.2	129.3
$R_f{}^a$	0.050	0.035
$R_w{}^b$	0.052	0.040
GOF^c	1.55	1.44

^{a} $R_f = \sum(|F_o| - |F_c|)/\sum(|F_o|)$. ^{b} $R_w = \{\sum w(|F_o| - |F_c|)^2/\sum(w|F_o|^2)\}^{1/2}$. ^{c} GOF $= \{\sum w(|F_o| - |F_c|)^2/(n - m)\}^{1/2}$; where n = number of reflections, m = number of refinement parameters.

Table 2. Positional and Thermal Parameters^a for $(H_2AETH)BiI_5$

atom	x	y	z	B_{iso} (Å^2)
Bi	0.13541(4)	0.30099(3)	0.2825(4)	3.10(4)
I(1)	0.22960(8)	0.30004(5)	−0.0210(4)	4.10(8)
I(2)	0.13458(9)	0.21585(5)	0.2696(4)	4.6(1)
I(3)	0.15027(9)	0.39135(5)	0.2966(5)	4.7(1)
I(4)	0.02693(8)	0.30780(6)	0.0582(4)	4.30(9)
I(5)	0.05646(8)	0.30376(5)	0.5698(4)	4.23(9)
S(1)	0.1903(4)	0.1290(3)	−0.015(2)	8.5(6)
S(2)	0.0824(5)	−0.0278(3)	0.117(1)	8.1(6)
N(1)	0.104(1)	0.2255(6)	−0.164(3)	4.7(5)
C(1)	0.164(1)	0.2109(8)	−0.243(4)	5.4(7)
C(2)	0.155(1)	0.169(1)	−0.291(4)	6.1(8)
C(3)	0.137(1)	0.1437(8)	−0.157(3)	4.5(6)
C(4)	0.078(2)	0.1309(9)	−0.109(4)	6.2(8)
C(5)	0.070(2)	0.111(1)	0.036(5)	8(1)
C(6)	0.130(2)	0.108(1)	0.101(5)	7.8(9)
C(7)	0.149(2)	0.087(1)	0.249(7)	11(1)
C(8)	0.097(2)	0.079(1)	0.343(7)	12(2)
C(9)	0.130(2)	0.058(1)	0.516(7)	12(1)
C(10)	0.078(3)	0.039(2)	0.587(8)	13(2)
C(11)	0.130(3)	0.027(2)	0.75(1)	18(2)
C(12)	0.084(3)	0.011(2)	0.824(8)	13(2)
C(13)	0.129(2)	−0.002(1)	0.979(5)	8(1)
C(14)	0.195(2)	−0.006(1)	1.021(5)	8(1)
C(15)	0.204(1)	−0.0286(9)	1.152(4)	5.4(7)
C(16)	0.150(2)	−0.044(1)	1.224(4)	6.3(9)
C(17)	0.141(2)	−0.069(1)	1.370(5)	8(1)
C(18)	0.124(1)	−0.109(1)	1.319(5)	6.9(9)
N(2)	0.175(1)	−0.1256(6)	1.209(3)	4.6(5)

^{a} The heavy atoms (Bi, I, and S) are refined anisotropically; anisotropic thermal parameters are listed in Table S.2 (Supporting Information).

Results and Discussion

Crystal Structures. The $(H_2AETH)BiI_5$ and $(H_2DDDA)BiI_5$ structures, as well as that previously determined[12] for (H_2DAH)-BiI_5, each consist of a framework of quasi-one-dimensional zigzag chains of distorted BiI_6 octahedra, separated by a network of diammonium organic cations (Figure 2). The inorganic chain structure for $(H_2AETH)BiI_5$ (Figure 3) is derived from a single crystallographically independent BiI_6 octahedron, with Bi−I bond lengths (Table 4) ranging from 2.942(3) to 3.233(3) Å and an average bond length of 3.087 Å. The long bridging Bi−I(1) bonds make up the backbone of the inorganic chain. The shortest terminal [Bi−I(4) and Bi−I(5)] bonds appear trans to these long interactions, and the two apical Bi−I(2) and Bi−I(3) bonds, which are cis to the long interactions, are intermediate in length. In addition to the bond length differences, the I−Bi−I bond angles (Table 4) deviate substantially from 90°,

Table 3. Positional and Thermal Parameters[a] for (H₂DDDA)BiI₅

atom	x	y	z	B_{iso} (Å²)
Bi	0.14087(2)	0.15707(1)	0.0	3.87(2)
I(1)	0.0	0.16766(3)	0.25	5.80(4)
I(2)	0.15823(5)	0.24470(2)	0.0	6.77(5)
I(3)	0.09876(6)	0.06881(3)	0.0	8.20(6)
I(4)	0.25029(3)	0.14934(2)	0.25725(6)	5.90(3)
N(1)	0.1085(9)	0.9121(4)	0.0	9.1(3)
N(2)	0.3608(8)	1.2734(4)	0.0	9.1(4)
C(1)	0.134(1)	0.9513(7)	0.0	11.9(6)
C(2)	0.215(2)	0.958(1)	0.0	17(1)
C(3)	0.262(3)	0.978(2)	0.0	24(2)
C(4)	0.344(2)	0.982(1)	0.0	19(1)
C(5)	0.339(2)	1.0216(9)	0.0	15.8(9)
C(6)	0.426(2)	1.0465(9)	0.0	16.2(9)
C(7)	0.451(3)	1.085(2)	0.0	25(2)
C(8)	0.519(2)	1.1057(9)	0.0	14.8(8)
C(9)	0.501(3)	1.149(2)	0.0	25(2)
C(10)	0.466(2)	1.176(1)	0.0	15.1(9)
C(11)	0.436(2)	1.214 (1)	0.0	15.2(9)
C(12)	0.390(2)	1.239(1)	0.0	18(1)

[a] The heavy atoms (Bi and I) are refined anisotropically; anisotropic thermal parameters are listed in Table S.3 (Supporting Information).

Table 4. Selected Bond Distances (Å) and Angles (deg) for (H₂AETH)BiI₅

Bi−I(1)	3.233(3)	I(1)[a]−Bi−I(4)	169.65(8)
Bi−I(1)[a]	3.230(2)	I(1)[a]−Bi−I(5)	91.91(7)
Bi−I(2)	2.989(2)	I(2)−Bi−I(3)	174.86(6)
Bi−I(3)	3.187(2)	I(2)−Bi−I(4)	93.02(7)
Bi−I(4)	2.942(3)	I(2)−Bi−I(5)	93.49(8)
Bi−I(5)	2.942(3)	I(3)−Bi−I(4)	90.89(7)
S(1)−C(3)	1.71(3)	I(3)−Bi−I(5)	89.30(8)
S(1)−C(6)	1.74(4)	I(4)−Bi−I(5)	97.46(8)
S(2)−C(13)	1.77(4)	Bi−I(1)−Bi[b]	157.9(1)
S(2)−C(16)	1.75(3)	C(3)−S(1)−C(6)	95(2)
N(1)−C(1)	1.49(4)	C(13)−S(2)−C(16)	95(2)
C(1)−C(2)	1.55(4)	N(1)−C(1)−C(2)	110(2)
C(2)−C(3)	1.49(4)	C(1)−C(2)−C(3)	112(3)
C(3)−C(4)	1.35(4)	S(1)−C(3)−C(2)	125(2)
C(4)−C(5)	1.43(6)	S(1)−C(3)−C(4)	105(2)
C(5)−C(6)	1.35(5)	C(2)−C(3)−C(4)	130(3)
C(6)−C(7)	1.52(7)	C(3)−C(4)−C(5)	121(3)
C(7)−C(8)	1.37(7)	C(4)−C(5)−C(6)	107(3)
C(8)−C(9)	1.79(8)	S(1)−C(6)−C(5)	111(3)
C(9)−C(10)	1.38(7)	S(1)−C(6)−C(7)	119(3)
C(10)−C(11)	1.8(1)	C(5)−C(6)−C(7)	128(4)
C(11)−C(12)	1.3(1)	C(6)−C(7)−C(8)	112(4)
C(12)−C(13)	1.67(8)	C(7)−C(8)−C(9)	106(4)
C(13)−C(14)	1.40(5)	C(8)−C(9)−C(10)	106(4)
C(14)−C(15)	1.39(6)	C(9)−C(10)−C(11)	89(4)
C(15)−C(16)	1.37(5)	C(10)−C(11)−C(12)	93(5)
C(16)−C(17)	1.53(5)	C(11)−C(12)−C(13)	97(5)
C(17)−C(18)	1.53(5)	S(2)−C(13)−C(12)	111(3)
C(18)−N(2)	1.53(4)	S(2)−C(13)−C(14)	107(3)
I(1)−Bi−I(1)[a]	84.85(8)	C(12)−C(13)−C(14)	139(3)
I(1)−Bi−I(2)	87.90(7)	C(13)−C(14)−C(15)	113(3)
I(1)−Bi−I(3)	89.07(7)	C(14)−C(15)−C(16)	118(3)
I(1)−Bi−I(4)	85.67(7)	S(2)−C(16)−C(15)	105(3)
I(1)−Bi−I(5)	176.49(7)	S(2)−C(16)−C(17)	121(2)
I(1)[a]−Bi−I(2)	90.80(6)	C(15)−C(16)−C(17)	133(3)
I(1)[a]−Bi−I(3)	84.79(6)	C(16)−C(17)−C(18)	108(3)
		C(17)−C(18)−N(2)	112(2)

[a] 0.5 − x, y, 0.5 + z. [b] 0.5 − x, y, −0.5 + z.

with the biggest difference [97.46(8)°] occurring for the I(4)−Bi−I(5) angle, which incorporates the two shortest Bi−I bonds. The 157.9(1)° Bi−I(1)−Bi angle along the chain reflects that the BiI₆ octahedra are also somewhat rotated relative to each other in the a−c plane (see Figure 3a).

The conformation of the (H₂AETH)²⁺ cation (Figure 4) helps to dictate how the chainlike BiI₅²⁻ anions are positioned relative to each other. Each thiophene ring is essentially planar, with

Table 5. Selected Bond Distances (Å) and Angles (deg) for (H₂DDDA)BiI₅

Bi−I(1)	3.2711(4)	I(1)[a]−Bi−I(2)	87.89(2)
Bi−I(1)[a]	3.2711(4)	I(1)[a]−Bi−I(3)	86.27(2)
Bi−I(2)	3.019(1)	I(1)[a]−Bi−I(4)	171.93(2)
Bi−I(3)	3.111(1)	I(1)[a]−Bi−I(4)[b]	89.13(2)
Bi−I(4)	2.9290(6)	I(2)−Bi−I(3)	172.20(3)
Bi−I(4)[b]	2.9290(6)	I(2)−Bi−I(4)	91.51(2)
N(1)−C(1)	1.41(3)	I(2)−Bi−I(4)[b]	91.51(2)
C(1)−C(2)	1.42(3)	I(3)−Bi−I(4)	93.56(2)
C(2)−C(3)	1.08(7)	I(3)−Bi−I(4)[b]	93.56(2)
C(3)−C(4)	1.42(7)	I(4)−Bi−I(4)[b]	98.93(2)
C(4)−C(5)	1.35(5)	Bi−I(1)−Bi[c]	167.26(3)
C(5)−C(6)	1.72(5)	N(1)−C(1)−C(2)	117(2)
C(6)−C(7)	1.38(6)	C(1)−C(2)−C(3)	147(4)
C(7)−C(8)	1.38(6)	C(2)−C(3)−C(4)	144(5)
C(8)−C(9)	1.53(6)	C(3)−C(4)−C(5)	92(3)
C(9)−C(10)	1.10(7)	C(4)−C(5)−C(6)	116(3)
C(10)−C(11)	1.41(6)	C(5)−C(6)−C(7)	137(3)
C(11)−C(12)	1.16(6)	C(6)−C(7)−C(8)	139(4)
C(12)−N(2)	1.28(4)	C(7)−C(8)−C(9)	109(3)
I(1)−Bi−I(1)[a]	82.81(1)	C(8)−C(9)−C(10)	158(5)
I(1)−Bi−I(2)	87.89(2)	C(9)−C(10)−C(11)	168(4)
I(1)−Bi−I(3)	86.27(2)	C(10)−C(11)−C(12)	158(3)
I(1)−Bi−I(4)	89.13(2)	C(11)−C(12)−N(2)	160(4)
I(1)−Bi−I(4)[b]	171.93(2)		

[a] −x, y, −0.5 + z. [b] x, y, −z. [c] −x, y, 0.5 + z.

all non-hydrogen atoms falling within 0.01(5) Å of the least-squares best plane. The hexane fragment between the thiophene rings is essentially all-trans with, however, larger thermal parameters [11(1) < B_{iso} < 18(2)] compared with those found in the rest of the organic molecule [4.5(6) < B_{iso} < 8(1)], suggesting that this component is more susceptible to either static or dynamic (thermal) disorder. The thiophene rings and the hexane connecting group are all to first approximation coplanar (all atoms are within 0.2 Å of the least-squares best plane). However, the two ethylammonium end groups clearly extend out of this plane (Figure 4), leading to an overall S-shape conformation when the cation is viewed from the side. This conformation is similar to that observed for the protonated 5,5‴-bis(aminoethyl)-2,2′:5′,2″:5″,2‴-quaterthiophene (AEQT) molecule in (H₂AEQT)PbBr₄.[2]

For (H₂AETH)BiI₅, the inorganic chains and (H₂AETH)²⁺ cations form alternating layers along the b axis (Figure 2a), with the inorganic layers consisting of a pseudo-two-dimensional array of BiI₅²⁻ chains (which extend along the c axis of the structure). Close interactions between iodides on adjacent chains include I(4)···I(2)′ [4.204 Å], I(5)···I(2)′ [4.316 Å], and I(5)···I(4)′ [4.269 Å], where the primed atoms are on a different chain from the unprimed atoms. These distances are slightly less than twice the ionic radius for the iodide ion (2.2 Å),[26] indicating that the chains are in close contact within the inorganic layers. In comparison, the intermolecular I···I distances in crystalline I₂ are 3.50 Å, 3.97 Å (in-layer), and 4.27 Å (between layers).[27] The (H₂AETH)²⁺ cations are substantially tilted relative to the crystallographic b axis when viewed down the a axis (Figure 5), with a dihedral angle between the best planes for the AETH molecule (excluding the ethylammonium groups) and the BiI₅²⁻ chain [defined using Bi, I(1), I(4), I(5)] of 28.6(1)°. Note that organic cations associated with each successive inorganic chain along the a axis alternate in the direction of tilt (Figure 5).

The (H₂DDDA)BiI₅ chain structure (Figure 6) exhibits a similar Bi coordination and range of Bi−I bond lengths

(26) Shannon, R. D. *Acta Crystallogr.* **1976**, *A32*, 751.
(27) van Bolhuis, F.; Koster, P. B.; Migchelsen, T. *Acta Crystallogr.* **1967**, *23*, 90.
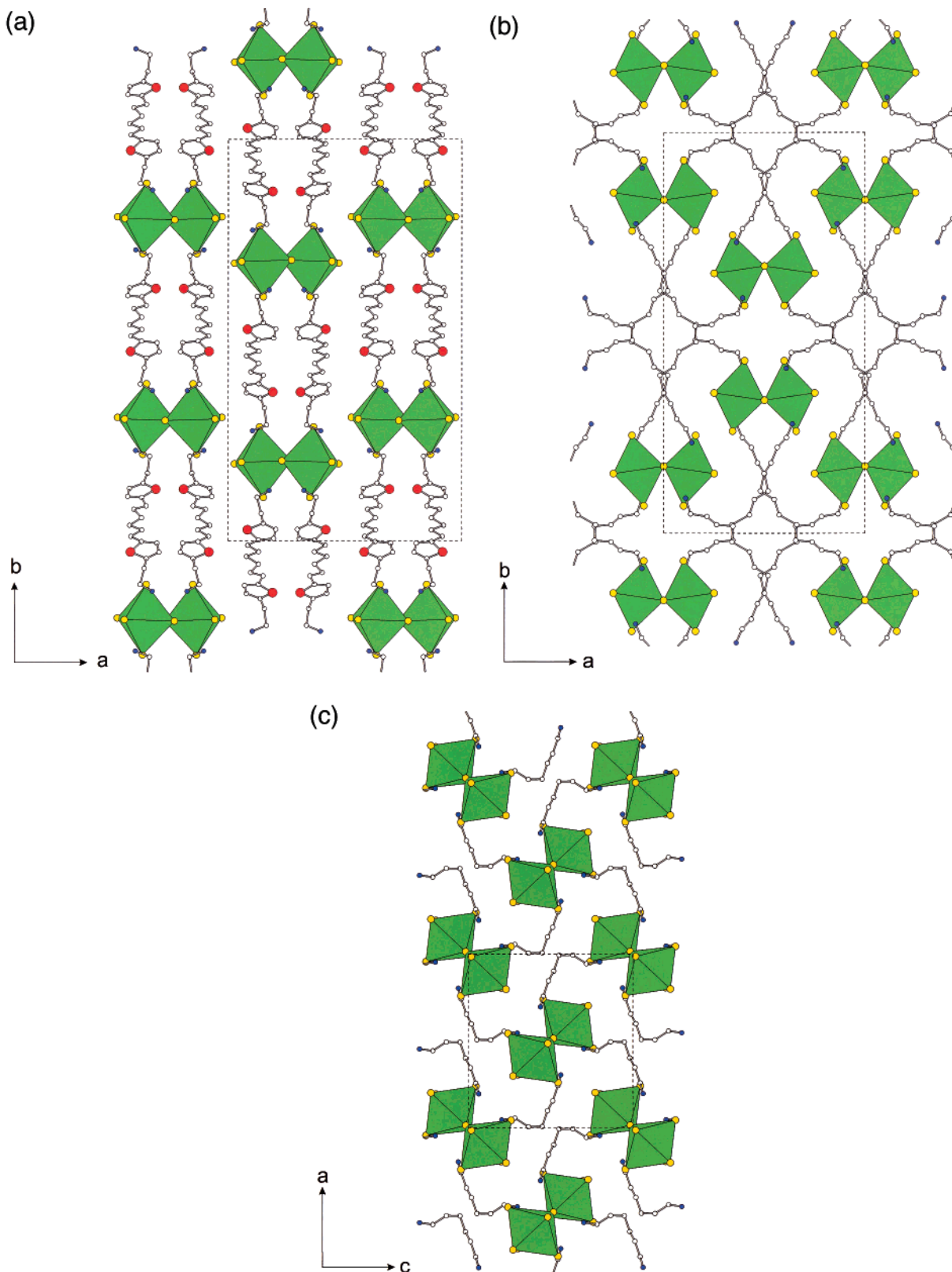
Figure 2. Crystal structures of (a) (H$_2$AETH)BiI$_5$, (b) (H$_2$DDDA)BiI$_5$, and (c) (H$_2$DAH)BiI$_5$, viewed down an axis parallel to the BiI$_5^{2-}$ chains (shown in polyhedral representation). Dashed lines depict the unit cell outline for each structure. For clarity, the atoms are represented as spheres with uniform sizes selected for each atom type.

compared with (H$_2$AETH)BiI$_5$ (Table 5), and essentially an identical average Bi–I bond length of 3.088 Å. The biggest I–Bi–I bond angle deviation (from 90°) occurs for the I(4)–Bi–I(4)^b angle (98.93°) which, as for the (H$_2$AETH)BiI$_5$ structure, involves the two shortest terminal Bi–I bonds. The

Bi–I(1)–Bi angle of 167.26(3)° is closer to 180° than for (H$_2$-AETH)BiI$_5$. The iodide thermal ellipsoids within the chains are larger than for the (H$_2$AETH)BiI$_5$ compound [especially the apical I(2) and I(3) iodides], suggesting that there may be more thermal motion for these ions. The thermal parameters for the
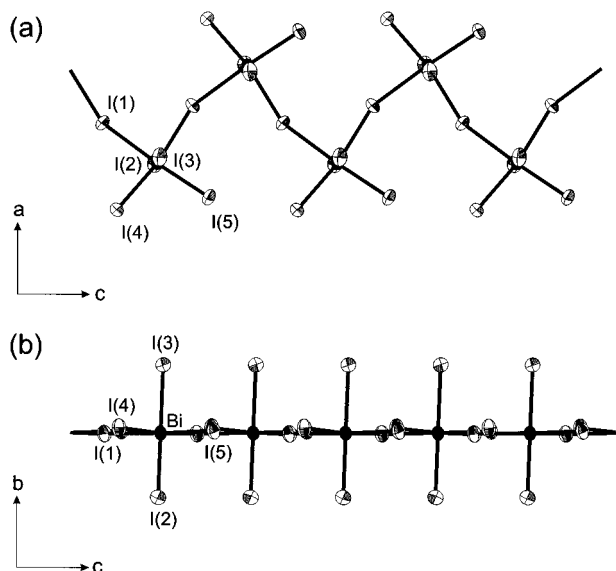
Figure 3. The $BiI_5{}^{2-}$ chain structure for $(H_2AETH)BiI_5$, viewed from the (a) top and (b) side. Atom labeling and thermal ellipsoids are given for the Bi and I atoms. The thermal ellipsoids are drawn at 50% probability.
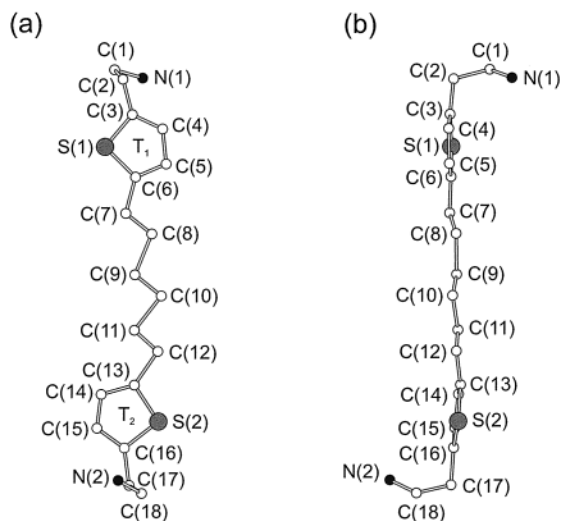

Figure 4. (a) Top and (b) side views of the doubly protonated 1,6-bis[5′-(2″-aminoethyl)-2′-thienyl]hexane (AETH) molecule in $(H_2$-$AETH)BiI_5$. For clarity, the atoms are represented as spheres with uniform sizes selected for each atom type.

DDDA molecules are also larger than for the AETH system. In addition, some carbon−carbon bond lengths and angles within the DDDA chain deviate from ideal values (e.g., C−C bond lengths >1.6 Å or <1.2 Å), further suggesting disorder within the alkyl chain. In contrast to the hexane segment in the AETH molecule, the aliphatic DDDA chain is not all trans. The bending of the DDDA molecule, along with the substantial disorder suggested by the refinement, reflects the substantial flexibility of this molecule.

As for $(H_2AETH)BiI_5$, the $(H_2DDDA)BiI_5$ structure can nominally be viewed (Figure 2b) as consisting of alternating layers of $BiI_5{}^{2-}$ chains and $(H_2DDDA)^{2+}$ cations, stacked along the *b* axis. Adjacent $BiI_5{}^{2-}$ chains in $(H_2AETH)BiI_5$ are displaced along the *b* axis by approximately one-half of the height of a BiI_6 octahedron (Figure 2a), leading to a slight corrugation or up−down alternation of these chains progressing along the *a* axis within each layer. In $(H_2DDDA)BiI_5$, the staggering of the chains is similar, with however a substantially
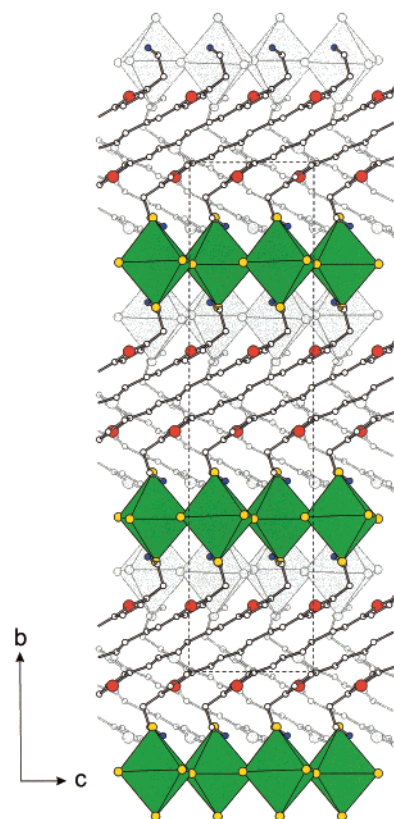
Figure 5. Crystal structure of $(H_2AETH)BiI_5$, viewed down the *a* axis. Dashed lines depict the unit cell outline. For clarity, the atoms are represented as spheres with uniform sizes selected for each atom type. In addition, the second group of $BiI_5{}^{2-}$ chains/$(H_2AETH)^{2+}$ cations from the front of the cell along the *a* axis is shown in gray outline to aid in distinguishing from the components closest to the front of the cell, and also to highlight the alternation in tilt direction of the $(H_2AETH)^{2+}$ cations.
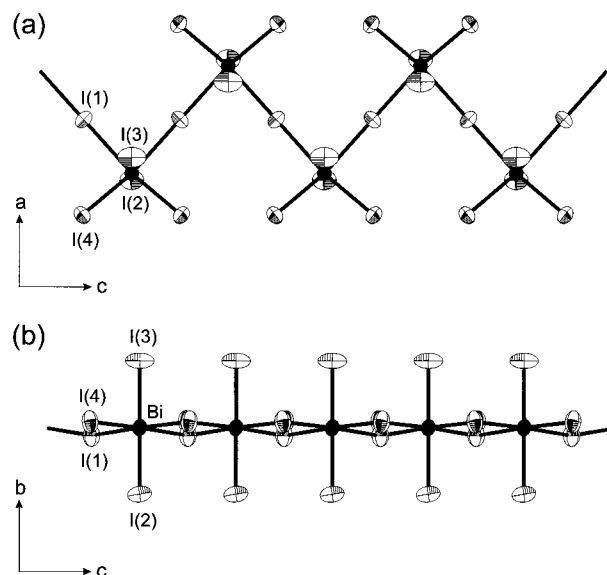
Figure 6. The $BiI_5{}^{2-}$ chain structure for $(H_2DDDA)BiI_5$, viewed from the (a) top and (b) side. Atom labeling and thermal ellipsoids are given for the Bi and I atoms. The thermal ellipsoids are drawn at 50% probability.

more pronounced displacement of the neighboring chains along the *b* axis (approximately the full height of a BiI_6 octahedron). This makes each layer of $BiI_5{}^{2-}$ chains more puckered than in the $(H_2AETH)BiI_5$ system. The close interactions between iodides on adjacent chains within a layer include I(4)···I(2)′

[4.482 Å], slightly larger than for (H$_2$AETH)BiI$_5$. Also, while the up−down alternation of the inorganic chains is in registry from layer to layer in the (H$_2$AETH)BiI$_5$ compound (i.e., with the "down chain" of one layer matching the "down chain" of each adjacent layer), the layers are out of phase in (H$_2$DDDA)-BiI$_5$, with the "down chain" of one layer matching the "up chain" of each adjacent layer. This leads to closer interaction [5.816 Å I(3)···I(3)′ distance] between chains in adjacent inorganic layers, making for a more three-dimensional packing.

A similar BiI$_5^{2-}$ chain structure has also recently been reported[12] for (H$_2$DAH)BiI$_5$ (Figure 2c), with Bi−I bond lengths ranging from 2.914(1) to 3.301(1) Å, and an average Bi−I bond distance of 3.099 Å. As for the new compounds reported above, the two long bridging bonds (3.301 and 3.260 Å) alternate down the length of the chain, with the two shortest interactions (2.914 and 2.957 Å) appearing trans to these bonds. Similarly, the biggest I−Bi−I bond angle deviation from 90° (99.93°) involves the two short terminal Bi−I bonds. The bridging Bi−I−Bi bond angle of 163.54(2)° is intermediate to the values found for the two title compounds.

Notice that, in the two new structures, the plane defined by each zigzag BiI$_5$ chain is approximately parallel to that for each nearest neighbor. In (H$_2$DAH)BiI$_5$, the planes of nearest neighbor chains are mutually orthogonal, leading to a more three-dimensional packing of the array of chains (Figure 2c). Close interactions between iodides on adjacent chains include I(4)···I(2)′ (4.458 Å). The nearest-neighbor interchain center-to-center distance is 10.45 Å, with these interactions extending along both cell diagonal directions in the *a*−*c* plane (Figure 2c). Similarly, the interchain distance within the inorganic layers of (H$_2$AETH)BiI$_5$ is 10.80 Å. However, the shortest interchain distance between inorganic layers is 17.35 Å, leading to a substantially more two-dimensional stacking. In (H$_2$DDDA)-BiI$_5$, the corresponding distances are 10.30 and 11.49 Å for interchain distances within and between the inorganic layers of the structure, leading to an intermediate case with regard to the layering of the chains.

By comparing the three BiI$_5^{2-}$ chain compounds, it is clear that the organic cation can have a substantial impact on the type of stacking achieved for, and therefore the degree of interaction between, the inorganic chains. The similarity in the inorganic chains for each of these compounds, despite the substantially different organic cations and packing, additionally indicates that this type of one-dimensional chain structure may be more generally encountered in the (H$_3$N−R−NH$_3$)BiI$_5$ family. It should be noted that other distinct inorganic structures are known for the BiX$_5^{2-}$ anion. In K$_2$BiBr$_5$·2H$_2$O, (NH$_4$)$_2$BiBr$_5$·2H$_2$O, and (HL)$_2$BiBr$_5$ (L = 2,5-diamino-1,3,4-thiadiazole), for example, the inorganic unit consists of isolated edge-sharing pairs of BiBr$_6$ octahedra.[28,29] In these cases, the inorganic bioctahedral anion is usually denoted as Bi$_2$X$_{10}^{4-}$.

Optical Properties. The substantial structural diversity of bismuth halogenoanions provides a range of model systems for examining the effect of inorganic framework bonding and dimensionality on electronic and optical properties. Kawai and Shimanuki,[30] for example, have examined the optical properties of (CH$_3$NH$_3$)$_3$Bi$_2$I$_9$ single crystals, which structurally consist of an array of face-sharing bioctahedral Bi$_2$I$_9^{3-}$ anions surrounded by the methylammonium cations. A clear exciton peak is observed at liquid nitrogen temperature with a peak wave-
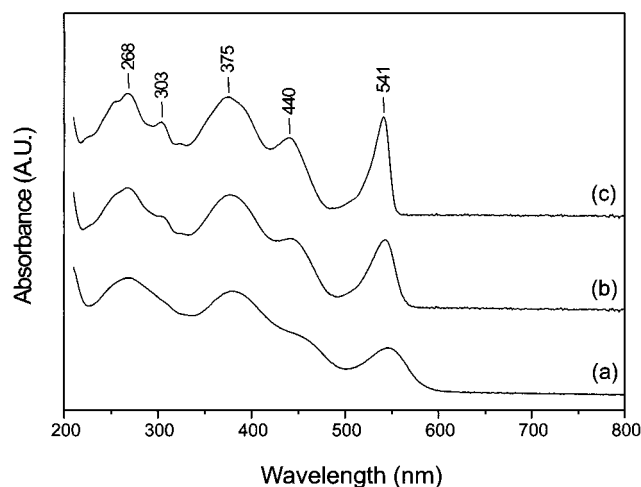
Figure 7. UV−vis absorption spectra for a thermally ablated thin film of (H$_2$DAH)BiI$_5$ on a sapphire substrate at (a) 290 K, (b) 130 K, and (c) 25 K. The positions of the spectral features (in nm) are noted in the low-temperature data.

length of 494 nm (2.51 eV). The peak is also observable at room temperature, indicating a large exciton binding energy (estimated to be ∼300 meV). In (C$_6$H$_5$C$_2$H$_4$NH$_3$)$_4$BiI$_7$·H$_2$O, which contains smaller isolated BiI$_6^{3-}$ octahedra, the exciton peak falls at slightly higher energy (474 nm).[11] For (H$_2$DAH)-BiI$_5$, with its extended BiI$_5^{2-}$ chains, the peak red-shifts to 554 nm,[12] while in the more two-dimensional BiI$_3$ structure, the direct exciton transition occurs at approximately 600 nm.[31] These results apparently reflect the effect of the inorganic framework dimensionality on the electronic structure of the material.[12] However, it is interesting to also consider the variations in the electronic structure within a given structural class of inorganic framework, produced by incorporating different organic cations.

In Figure 7, the absorption spectra for a thermally ablated (H$_2$DAH)BiI$_5$ thin film are shown as a function of temperature. At room temperature (Figure 7a), the spectrum is very similar to that reported by Mousdis et al.[12] for deposits of the same compound on quartz (prepared from solution or from rubbing crystals of the compound on the quartz plate in the presence of acetone). The exciton band in the current SSTA-deposited film appears at slightly shorter wavelength (547 nm) relative to the previous study (554 nm), perhaps as a result of a smaller grain size for the ablated film. A grain size dependence of the exciton band position has been previously noted for SSTA-deposited (H$_2$AETH)PbI$_4$ films, where the spectral peak position exhibits a shift of about 30 nm as a result of different film annealing conditions.[22] Note that, at room temperature, the exciton band is substantially broadened. At lower temperatures (Figure 7b,c), the peak shifts slightly to smaller wavelength (541 nm at 25 K), increases in intensity, and becomes substantially sharper, making it easier to distinguish from the continuum absorption.

The corresponding spectra for (H$_2$AETH)BiI$_5$ and (H$_2$-DDDA)BiI$_5$ are shown in Figures 8 and 9, respectively. Despite the very similar inorganic chain structure, the exciton band in (H$_2$AETH)BiI$_5$ occurs at substantially higher energy (λ_{ex} = 491 nm at 25 K) compared with that found in (H$_2$DAH)BiI$_5$. This spectral difference is also clearly evident when observing powders of the two materials. Whereas (H$_2$AETH)BiI$_5$ powders are light red (with a slight orange hue), (H$_2$DAH)BiI$_5$ powders are dark red in appearance. Note that the exciton band peak position in (H$_2$AETH)BiI$_5$ is similar to that observed for the

(28) Lazarini, F. *Acta Crystallogr.* **1977**, *B33*, 1954.
(29) Benedetti, A.; Fabretti, A. C.; Malavasi, W. *J. Crystallogr. Spectrosc. Res.* **1992**, *22*, 145.
(30) Kawai, T.; Shimanuki, S. *Phys. Status Solidi B* **1993**, *177*, K43.

(31) Kaifu, Y. *J. Lumin.* **1988**, *42*, 61.
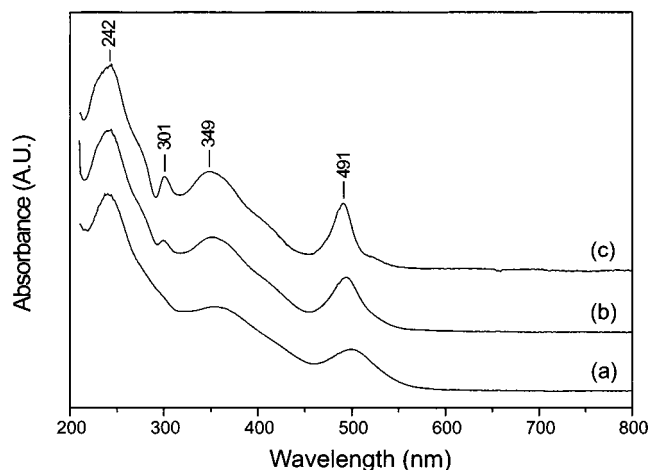
Figure 8. UV−vis absorption spectra for a thermally ablated thin film of (H₂AETH)BiI₅ on a sapphire substrate at (a) 290 K, (b) 130 K, and (c) 25 K. The positions of the spectral features (in nm) are noted in the low-temperature data.
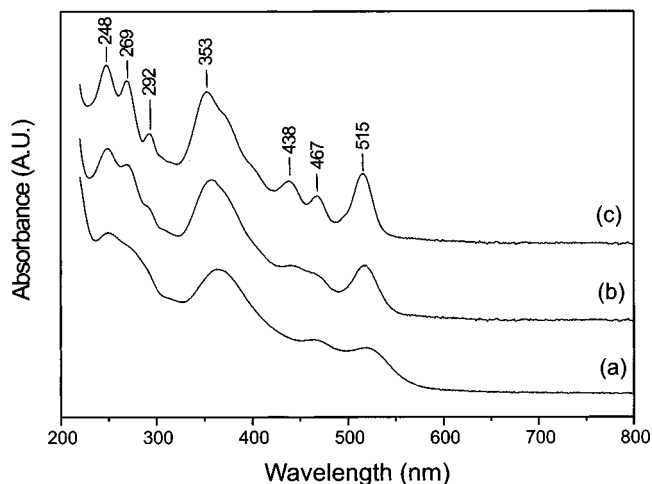
Figure 9. UV−vis absorption spectra for a thermally ablated thin film of (H₂DDDA)BiI₅ on a sapphire substrate at (a) 290 K, (b) 130 K, and (c) 25 K. The positions of the spectral features (in nm) are noted in the low-temperature data.

isolated bioctahedral $Bi_2I_9^{3-}$ anions,[30] indicating that the band positions are substantially influenced by more than just the effective dimensionality of the inorganic framework. The long-wavelength spectral feature in (H₂DDDA)BiI₅ is intermediate in position to that observed in (H₂DAH)BiI₅ and (H₂AETH)-BiI₅ (515 nm at 25 K).

As discussed above, the BiI_5^{2-} chain structures for (H₂DAH)-BiI₅, (H₂AETH)BiI₅, and (H₂DDDA)BiI₅ are very similar, with the BiI_6 octahedra exhibiting a comparable range of distortion for the three compounds. While there are more significant differences in the Bi−I−Bi bond angles along the BiI_5^{2-} chains (157.9−167.3°), there is no apparent correlation between this angle and the position of the bands in the optical spectra. It is therefore likely that the distinctions among the optical spectra at least partially arise for reasons other than the slight differences in the extended BiI_5^{2-} anion structure. One possibility is to associate shifting in the exciton band position to differences in the effective dielectric constant of the organic layer surrounding the chains. In the (R−NH₃)₂PbI₄ perovskites, for example, the system containing an aromatic $C_6H_5C_2H_4NH_3^+$ moiety exhibits a smaller exciton binding energy compared to the system with an aliphatic $C_{10}H_{21}NH_3^+$ cation.[32] This spectral difference is attributed to the larger dielectric constant of the aromatic versus

the aliphatic species surrounding the inorganic sheets, thereby leading to an enhancement of screening between the electron and hole. However, the two aliphatic cations in (H₂DAH)BiI₅ and (H₂DDDA)BiI₅ are expected to provide a very similar dielectric environment for these two systems, despite the substantial shift in the spectral features.

There are also relatively close I···I interactions (4.2−4.5 Å) among the BiI_5^{2-} chains within each structure, with the interactions being primarily two-dimensional in (H₂AETH)BiI₅, three-dimensional in (H₂DAH)BiI₅, and intermediate in the case of (H₂DDDA)BiI₅. These inter-iodide distances correspond to approximately twice the ionic radius of an iodide ion, indicating that the chains are in close contact with each other along the directions of these interactions. The distances between chains are also comparable to the expected exciton radii (of order 10 Å) in the hybrid structures.[3] It is therefore likely that, while the dimensionality and detailed bonding of the inorganic framework are important in establishing the electronic and optical properties of an organic−inorganic hybrid, the interactions between neighboring inorganic moieties must also play an important role. Note that the interactions between chains may influence both the underlying electronic structure and the degree of exciton confinement within the material.

Conclusion

One mission of solid-state chemists is to identify and understand commonly occurring structural motifs within interesting classes of materials. In this report, two new (H₃N−R−NH₃)BiI₅ organic−inorganic hybrids have been identified: (H₂AETH)BiI₅ and (H₂DDDA)BiI₅. The $(H_2AETH)^{2+}$ and $(H_2\text{-}DDDA)^{2+}$ cations are longer and/or more complex than the 1,6 diammonium hexane cation, $(H_2DAH)^{2+}$, reported in (H₂DAH)-BiI₅,[12] suggesting that the structural motif of BiI_5^{2-} zigzag chains, observed previously in (H₂DAH)BiI₅, may be more generally observed among the bismuth(III) iodide based hybrids. Each of the three compounds listed above contains analogous chains of corner-sharing distorted BiI_6 octahedra. The range of Bi−I bond lengths is similar for the three compounds, with the longest Bi−I bonds (3.23−3.30 Å) running along the BiI_5^{2-} chains (i.e., the bridging bonds) and the shortest bonds (2.91−2.94 Å) appearing trans to these bonds. The apical Bi−I bonds are, in each case, intermediate in length (2.99−3.19 Å).

While the structures of the inorganic chains are alike for the three compounds, the different organic moieties result in markedly different packing configurations for the chains. These differences are brought about by the different steric constraints imposed by the organic cations (e.g., differences in length, shape, degree of flexibility), as well as by the interactions between the organic cations and the inorganic framework (e.g., hydrogen bonding and ionic forces between the ammonium end groups and the iodides) and among the organic cations themselves (e.g., van der Waals and aromatic−aromatic interactions). In this study, the differences in packing arrangements are expected to lead to more two-dimensional [as in (H₂AETH)BiI₅] or more three-dimensional [as in (H₂DAH)BiI₅] interactions between the inorganic chains. The (H₂DDDA)BiI₅ structure is intermediate in character between these two extremes. It is interesting to consider how these differences imposed by the various organic cations affect the properties of the resulting materials.

The dominant long-wavelength feature in the optical spectra for each of the three compounds has been attributed to an exciton band, which derives from the inorganic component of the

(32) Hong, X.; Ishihara, T.; Nurmikko, A. V. *Phys. Rev. B* **1992**, *45*, 6961.

structure. The position of this band shifts from 491 nm for $(H_2\text{-}AETH)BiI_5$ to 541 nm for $(H_2DAH)BiI_5$, with the position for $(H_2DDDA)BiI_5$ appearing intermediate between these two extremes. Note that this shift in energy (0.23 eV) is quite substantial and is similar in magnitude to the shift attributed to progressing between various effective dimensionalities (0D ↔ 1D ↔ 2D ↔ 3D) for the bismuth(III) halide framework.[12] These results therefore stress the likely importance of interactions between the inorganic moieties in understanding the electronic and optical properties of organic−inorganic hybrids containing lower-dimensional inorganic frameworks. Theoretical modeling of the effect of interchain interactions would be useful for a more complete understanding of the spectral differences observed among the reported $BiI_5{}^{2-}$ chain compounds.

Supporting Information Available: Tables providing a full listing of experimental and crystallographic data (Table S.1) and anisotropic temperature factors for $(H_2AETH)BiI_5$ (Table S.2) and $(H_2DDDA)\text{-}BiI_5$ (Table S.3). This material is available free of charge via the Internet at http://pubs.acs.org.